Taylor & Francis
Taylor & Francis Group

Cybernetics and Systems
An International Journal

ISSN: (Print) (Online) Journal homepage: https://www.tandfonline.com/loi/ucbs20

ODMNet: Automated Glaucoma Detection and Classification Model Using Heuristically-Aided Optimized DenseNet and MobileNet Transfer Learning

Felix Joseph Xavier & Fanax Femy F.

To cite this article: Felix Joseph Xavier & Fanax Femy F. (2023): ODMNet: Automated Glaucoma Detection and Classification Model Using Heuristically-Aided Optimized DenseNet and MobileNet Transfer Learning, Cybernetics and Systems, DOI: 10.1080/01969722.2023.2166250

To link to this article: https://doi.org/10.1080/01969722.2023.2166250

Published online: 03 Feb 2023.

CYBERNETICS AND SYSTEMS: AN INTERNATIONAL JOURNAL
https://doi.org/10.1080/01969722.2023.2166250

ODMNet: Automated Glaucoma Detection and Classification Model Using Heuristically-Aided Optimized DenseNet and MobileNet Transfer Learning

Felix Joseph Xavier[a] and Fanax Femy F.[b]

[a]Department of Electrical and Electronics Engineering, Bethlahem Institute of Engineering, Karungal, India; [b]Department of Computer Science, Holy Cross College (Autonomous), Nagercoil, India

ABSTRACT

In various existing works, glaucoma detection is not predicted accurately, which may lead to irreversible vision loss. A new framework is designed for detecting glaucoma by transfer learning approach. In the initial stage, the source images are gathered from standard datasets. After collecting the raw images, it is fed for image enhancement, performed through the Retinex approach. Further, the segmentation process is carried out by Modified DeepLabV3, where the significant Regions of Interest (ROI) are extracted by enhanced images and segmented the abnormalities. To meet the optimal value, the parameters in DeepLabV3 are tuned optimally by the Improved Rain Optimization Algorithm (IROA). Once the image is segmented, it is subjected to the detection or classification task, where the glaucoma is effectively classified by the hybrid learning method called Optimized DenseNet and MobileNet Transfer Learning (ODMNet) that is constructed with Densely Connected Convolutional Networks (DenseNet) and MobileNet, where the layers are optimized by IROA approach. Finally, the performance is assessed with the assistance of diverse metrics. In experimental analysis, the accuracy and F1-score of the designed method attain 96% and 93%. The recommended detection model achieves higher detection performance in telemedicine and healthcare applications.

KEYWORDS

Abnormality segmentation; automated glaucoma detection; improved rain optimization algorithm; modified DeepLabV3; optimized DenseNet and MobileNet transfer learning; retinex-based image enhancement

1. Introduction

Glaucoma is one of the major causes of irreversible blindness worldwide (George et al. 2020). Generally, the eye is categorized into glaucomatous and non-glaucomatous eyes by considering the characteristics of the eye. Blind spots developed in the glaucoma eye while observing the damage to optic nerve fibers (Islam et al. 2022). However, until noticing the damage to the optic nerve, the blind spots cannot be detected (Civit-Masot et al.

CONTACT Felix Joseph Xavier felixjoseph75@gmail.com Department of Electrical and Electronics Engineering, Bethlahem Institute of Engineering, Karungal, Tamilnadu, India.

2020). Here, early identification and treatment are mainly required to prevent vision loss. Generally, the intraocular pressure in the eye causes glaucoma through a malformation or malfunction of the eyes (Kim et al. 2013). This disorder is further classified into Primary Angle Closer Glaucoma (PACG) and Primary Open-Angle Glaucoma (POAG) (Li et al. 2020). Here, PACG is generally asymptomatic and chronic, which leads to redness, nausea, frequent eye pain, and blurred vision. On the other hand, POAG is also painless and often has no symptoms until increased the damage of the disease and intends to grow slowly with time (Yousefi et al. 2014). More specifically, as the impact of glaucoma is consistently grown, the vision of the affected eye is permanently damaged. Consequently, it is complicated to identify the early stages until the situation is at a complicated phase (Parashar and Agrawal 2020). Therefore, there is a need for consistent eye examinations for early detection and prevention of glaucoma to get better results. Moreover, glaucoma is time-consuming for manual identification, costly, and subjective, and it notices higher differentiation in physician performances. Thus, the necessity of designing mode is suitable and efficient automated glaucoma detection models.

Generally, glaucoma has diverse classes like etcetera, normal tension, congenital, close-angle, and open-angle. For the early detection and treatment of glaucoma, there is no proper medical tool (Parashar and Agrawal 2021b). Though, recent technologies provide a way to stop the growth of glaucoma. Thus, to assist in the diagnosis and treatment of glaucoma patients, computer-aided diagnostic systems are required for treating severe conditions and also for better decision-making (Tabassum et al. 2020). Some recent approaches utilized for glaucoma detection models are up-to-disc ratio (CDR) measurement, laser ophthalmoscopy, Optical Coherence Tomography (OCT), Vertical Cup-Disc Ratio (VCDR), Spectral Domain OCT (SDOCT), Gonioscopy, Pachymetry, Tonometry, and so on (Niwas et al. 2016). Nowadays, various research approaches to glaucoma detection are recommended, which, however, do not offer satisfactory and consistent results (Cheng et al. 2013). These studies use color fundus images, generally processed by standard image processing techniques. Thus, the implementation of automatic glaucoma detection models has often achieved considerable inspiration for making reliable and faster decisions (Acharya et al. 2011). Some of the limitations in the existing glaucoma detection approaches are a lack of efficient pre-processing techniques for precise segmentation and a lack of better segmentation approaches for addressing the over or under-segmentation problems regarding the low contrast and existence of exudates among the boundaries. Thus, this research work adopts efficient pre-processing and segmentation techniques for offering better results on glaucoma detection.

Recent studies have recommended various approaches, including deep learning and heuristic approaches, for detecting glaucoma by processing optical fundus images (Afolabi et al. 2021). The digital fundus images are complicated owing to the irregularities in the gathered eye fundus images. It is a tiresome, time-consuming, and complicated problem. These techniques, however, use learning and segmentation-based techniques for exploring the relevant information from the images to illustrate the most representative capacity. As those approaches use hand-crafted features for the detection process, they suffer from a lack of adequate discriminative illustrations and also easily suffer from low contrast quality and pathological regions (Ma, Fallahzadeh, and Ghasemzadeh 2016). Deep learning methods are emerging to yield better representations in various fields. Thus, the recent glaucoma detection methods use deep learning methods to maximize the detection rate. Some standard deep learning approaches in this field are Artificial Neural Network (ANN) (Ambati et al. 2020), Convolutional Neural Network (CNN), Support Vector Machine (SVM), k-Nearest Neighbor (k-NN), etc. (Alghamdi and Abdel-Mottaleb 2021). However, the existing approaches are suffered from handling the diverse quality of images acquired by various equipment. These techniques take more computational time and resources (Guo et al. 2018). Thus, the emergence of transfer learning approaches in recent years grabs the attention of researchers in various fields. The recently suggested transfer learning approaches are ResNet-50, GoogLeNet, VGG, AlexNet, and so on (Luo et al. 2021). Hence, this research explores diverse transfer learning models for promoting glaucoma detection models.

The research points are discussed here.

- To implement ODMNet for automatic glaucoma detection and classification model using heuristically-aided transfer learning to maximize the detection rate for assisting the ophthalmologists in treating patients in preventing permanent vision loss.
- To derive a new Modified DeepLabV3 for extracting the significant Regions of Interest (ROI) from the pre-processed images and segmenting the abnormalities. Here, the Modified DeepLabV3 is suggested using the IROA algorithm by optimizing the parameters in DeepLabV3. It increases detection accuracy by precisely segmenting the abnormalities in the images.
- To design an IROA algorithm for implementing better segmentation and detection approaches, where the parameters in DeepLabV3 for better abnormality segmentation and the parameters in DenseNet and MobileNet for precise detection of glaucoma are tuned.
- To propose a new hybrid transfer learning method with the adoption of DenseNet and MobileNet techniques along with the IROA algorithm,

known as ODMNet, for glaucoma detection and classification model automatically for increasing the accuracy and precision rate in detected outcomes.

The residual modules in the recommended technique are illustrated below. Module II shows the conventional research works on glaucoma detection. Module III recommends advancing a new deep learning model for computer-aided glaucoma detection and classification. Module IV specifies image enhancement and optimized DeeplabV3 for abnormality segmentation. Module V illustrates the modified DenseNet and MobileNet with architecture optimization for glaucoma detection and classification. Module VI estimates the results. Module VII completes this paper.

2. Conventional Research Works on Glaucoma Detection

2.1. Related Works

Li et al. (2020) have designed a glaucoma detection model using an Attention-based CNN. Here, the data was gathered from the Large-Scale Attention-Based Glaucoma (LAG) database that has contained 11,760 fundus images for both negative and positive glaucoma classes. Moreover, the Attention-based CNN was utilized to perform the glaucoma classification along with the attention maps of eye-tracking experiments. Then, they predicted the attention maps for highlighting the salient regions for detecting glaucoma via weakly supervised training. The localized pathological regions were visualized to maximize the performance of glaucoma detection. The suggested system has finally ensured superior performance over other conventional methods.

Song, Lai, and Su (2021b) have recommended a new method with Retinex theory, Design of Experiment (DOE), and generalized loss function along with CNN for enhancing the results of gathered fundus images by eradicating the light effects through restoring the original colors. The automatic glaucoma detection model has enhanced its performance regarding simplicity and effectiveness. From the overall analysis, the recommended work has achieved significant efficiency regarding robustness by evaluating with standard error metrics. Finally, the mathematical notations and intuitive graphs were formulated for the designed model and exhibited their efficacy in terms of results. Thus, this model was more applicable for detecting glaucoma in real time.

Parashar and Agrawal (2021a) have implemented a new 2-D Compact Variation Mode Decomposition (2-D-C-VMD) algorithm for classifying glaucoma stages, including advanced stage, early-stage, and healthy. This research work has adopted the pre-processing and decomposed via 2-D-C-

VMD and obtained various Variational Modes (VMs). Then, the features were attained from the initial VM via techniques like Fractal Dimension, Energy, Yager Entropy, Shannon Entropy, Renyi Entropy, and KapurEntropy (KE). Next, the dimensionality reduction was carried out via Linear Discriminant Analysis (LDA). At last, the classification was performed via a trained Multiclass Least-Squares-Support Vector Machine (MC-LS-SVM) classifier. The estimation was performed via tenfold cross-validation and analyzed by differentiating it from other approaches.

Parashar and Agrawal (2021b) have recommended a Two-Dimensional Tensor Empirical Wavelet Transform (2D-T-EWT). This technique was applied to pre-processed images for performing the image decomposition to get Subband Images (SBIs). Next, the features were attained using moment-invariant, chip histogram, and Grey Level Co-Occurrence Matrix (GLCM). Next, the selection of reliable features was done and then ranked via the student's *t* test algorithm. At last, the trained MC-LS-SVM classifier was utilized to get the final classification outcomes. The performance of the designed model was enhanced via the glaucoma classification via tenfold cross-validation and attained superior outcomes over others.

Ovreiu, Paraschiv, and Ovreiu (2021) have designed a glaucoma identification model via CNNs to promote the medical field and assist ophthalmologists in offering early detection of diseases. A novel approach called DenseNet was recommended with 201 layers that were firstly pre-trained on ImageNet. This model was estimated over the ACRIMA dataset and has increased the efficiency regarding several performance metrics. Thus, finally, the suggested model has illustrated its significance in recognizing the identification of glaucoma. Serener and Serte (2019) have designed an automated glaucoma detection model using fundus images, where the classification was done by training deep CNN, ResNet-50, and GoogLeNet algorithms, and then, finally, the classification was carried out by fine-tuning the transfer learning model. Through evaluating the proposed model, the GoogLeNet model has achieved superior performance over others in detecting glaucoma and resulted in better efficiency.

Patel and Singh (2021) have used CNN for detecting the illness, and the individual patterns in the eye images were predicted via the Mask Region-Based Convolutional Neural Network (Mask-RCNN). It has created a hierarchical framework to differentiate the images among non-affected and glaucoma-affected eyes, which has assisted in better classification of glaucoma in patients. This model has estimated over 33 convolutional layers and six diverse degrees of complexity. The proposed approach has used a dropout strategy for maximizing the performance of glaucoma detection using ORIGA and SCES datasets and clearly illustrated the efficiency over other approaches.

Nayak et al. (2021) have presented a new approach termed Evolutionary Convolutional Network (ECNet) and Ensemble learning for glaucoma detection with the use of non-handcrafter feature extraction approaches. The discriminative features were extracted via several layers like convolutional, compression, Rectified Linear Unit (ReLU), and summation layer. The weights at diverse layers were optimized using a Real-Coded Genetic Algorithm (RCGA). A new criterion was suggested for training the ECNet to minimize the intra-class variance and maximize the inter-class distance of various classes. The gathered feature vectors were then fed to a set of classifiers like K-Nearest Neighbor (KNN), Backpropagation Neural Network (BPNN), Support Vector Machine (SVM), Extreme Learning Machine (ELM), and Kernel ELM (K-ELM) for getting better classification outcomes. The evaluation was done using the SVM with ECNet model that has achieved a higher accuracy rate while estimating with traditional approaches. This model has exhibited better screening in the real field.

Elangovan and Nath (2021) have designed a CNN for detecting the malaria parasite using thin blood smear images. Here, various performance metrics were evaluated to ensure the better performance of the networks. Thus, the empirical analysis of the recommended framework has achieved superior performance.

Nath and Dandapat (2012) have developed a novel Differential Entropy (DE) method for evaluating glaucoma. Moreover, 54 images were considered to detect glaucoma in the designed method. The result analysis of the developed model has proved that the better performance.

Kar, Neog, and Nath (2022) have implemented the Generative Adversarial Network (GAN) for analyzing the various loss functions. Here, the blood vessels were segmented with the help of GAN to predict the accurate outcome. Moreover, the contrast of blood vessels was improved by the histogram equalization algorithm. Thus, the experimental outcome of the proposed mechanism has obtained improved performance in terms of accuracy.

Shyamalee and Meedeniya (2022b) have implemented various CNN methods such as Inception-v3, Visual Geometry Group 19 (VGG19), and RNN-50 for classifying glaucoma with the help of eye fundus images. Moreover, the designed method was used to solve the overfitting issues and maximize the accuracy rate. Thus, the empirical analysis of the recommended framework has attained superior performance.

Shyamalee and Meedeniya (2022c) have designed the U-Net models along with the three CNN architectures for segmenting the fundus image. Here, various data augmentation was utilized to eliminate the overfitting problems. Thus, the empirical analysis of the U-Net model has achieved superior performance when combined with other traditional methods.

Shyamalee and Meedeniya (2022) have developed a novel computational method for segmenting and classifying the retinal fundus images to detect glaucoma in an automated way. Moreover, data augmentation techniques were used to improve the clarity of the retinal fundus image. Moreover, the segmentation and classification method was utilized by CNN architecture. Additionally, the RIM-ONE dataset was used to improve the accuracy. Throughout the analysis, the empirical of the suggested framework has attained enriched performance.

Venugopal et al. (2022a) have developed an effective Deep Threshold Prediction Network (DTP-Net) model for localizing the lesions on dermatological macro-images. Moreover, the grayscale version of the input images was fed into this model. Moreover, it can predict the threshold values. Thus, the empirical analysis of the DTP-Net has attained better performance over various meta-heuristic algorithms.

Venugopal et al. (2022a) have implemented an EfficientNet-based modified sigmoid transform to improve the contrast of the images. The transfer learning model was utilized to minimize the training time and dataset size. Hence, the sigmoid transform was used in the HSV color space. Thus, the result analysis of the proposed mechanism has higher performance than other-state-of-art-methods.

2.2. Problem Definition

Glaucoma is a non-curable eye disease acquired worldwide. Early detection and treatment can cure glaucoma, but due to the presence of very low qualified ophthalmologists, analysis becomes highly complex. Various techniques implemented for the classification and detection of glaucoma are listed in Table 1. AG-CNN (Li et al. 2020) utilized the subnet for classification, prediction, and localization. But it trained the data in a weakly supervised manner. CNN (Song, Lai, and Su 2021b) enhances the performance of effectiveness and robustness. Still, it contains a large amount of time, and also it is costly. MC-LS-SVM (Parashar and Agrawal 2021a) is fully adaptive and sharps the boundaries of fundus images. Yet, it can analyze only a limited dataset. MC-LS-SVM (Parashar and Agrawal 2021b) has very low computational complexity and provides high effectiveness. It highly needs to enhance the effectiveness of the classification rate. CNN (Ovreiu, Paraschiv, and Ovreiu 2021) was utilized to attain the closest ideal classifier value in the system. Even it didn't fit perfectly in some conditions due to different assumptions presented in the data. Resnet 50 and GoogLeNet (Serener and Serte 2019) use a fine-tuned sample set for a better performance rate and provide a highly accurate outcome. However, it is very expensive the identification of severity level. CNN (Patel and Singh 2021)

Table 1. Features and challenges of Glaucoma Detection and Classification based on Deep Learning.

Reference	Methodology	Features	Challenges
Li et al. 2020	AG-CNN	• It utilized the subnet for classification, prediction, and localization.	• It trained the data in a weakly supervised manner.
Song, Lai, and Su 2021b	CNN	• It improves the performance of effectiveness and robustness.	• It has high maintenance costs, and also it consumes more amount of time.
Parashar and Agrawal 2021a	MC-LS-SVM	• It is fully adaptive and sharps the boundaries of fundus images.	• It can analyze only limited datasets.
Parashar and Agrawal 2021b	MC-LS-SVM	• It has very low computational complexity and provides high effectiveness.	• It highly needs to improve the performance of the classification rate.
Ovreiu, Paraschiv, and Ovreiu 2021	CNNs	• It is utilized to attain the closest superior classifier value in the system.	• They didn't fit perfectly in some conditions due to different assumptions presented in the data.
Serener and Serte 2019	Resnet 50, GooLeNet	• It uses a fine-tuned sample set for a better performance rate and provides a highly accurate outcome.	• It is very expensive the identification of severity levels.
Patel and Singh 2021	CNN	• It utilized tuned and trained data for accurate classification.	• It makes the system complex when a huge amount of data is used.
Nayak et al. 2021	Ensemble	• It will automatically predict different severity levels presented in the individuals.	• It didn't provide an effective result when a small sample set was utilized.

utilized tuned and trained data for accurate classification. But, it makes the system complex when a huge amount of data is used. Ensemble (Nayak et al. 2021) automatically predicted different severity levels presented in the individuals. Yet, it didn't provide an effective result when a small sample set was utilized. The above limitations are considered and motivated to develop new glaucoma detection and classification model based on a deep learning mechanism.

3. Advancement of a New Deep Learning Model for Computer-Aided Glaucoma Detection and Classification

3.1. Proposed Glaucoma Detection Framework

Glaucoma is a major threat as it causes permanent vision loss, and thus, there is a need to predict it in an early manner (Liao et al. 2020; Ambati et al. 2020). For this purpose, computer-aided models have been emerging in recent studies. Although several studies are recommended for automated segmentation and classification of iris images, it requires performance improvement. The existing machine-learning approaches are suffered from higher processing time and computational complexity and also, and it does

not perform well on samples owing to the complicated image processing (Mary, Rajsingh, and Naik 2016). Here, deep learning plays a major role in detecting glaucoma as it has shown considerable performance over classification tasks (Vermeer et al. 2006; Soni et al. 2022). Even though deep learning performs well on detection tasks, it faces complications regarding code complexity and lack of generalization performance (Chan et al. 2002). They are also not applicable for varied attributes of glaucoma-affected areas. Thus, it is observed that the detection accuracy must be enhanced while detecting the glaucoma-affected regions (Bojja, Liu, and Sai Ambati 2021). As an extension to this deep learning, transfer learning techniques are suggested for promoting the medical image processing field. However, appropriate processing steps are required to avoid generalization errors (Song et al. 2021a). Moreover, the complicated nature of glaucoma lesions, including structure, color, and size differentiation, increases the complications in identifying glaucoma (Maheshwari, Pachori, and Acharya 2017). A precise model is required for classifying the lesions of glaucoma under the occurrence of various modifications in texture, color, and volume of lesions. It also must withstand blurring, noise effects, and also intensity variations in the gathered samples (Abdullah et al. 2021). Some common challenges noticed in the traditional glaucoma detection methods are not reliable in processing blurry images, lack of classification efficiency (Zhao et al. 2020), not strong color differentiation of the images, requiring larger training data, lack of detection accuracy owing to lower quality of gathered fundus images, computationally inefficient, needs additional processing power, economically expensive, and suffers from processing noisy images (Bojja et al. 2021; Nawaz et al. 2022). Hence, to eradicate the issues in the traditional works, this work tries to implement a new glaucoma detection framework using a heuristically-aided optimized transfer learning approach. The architecture of the designed ODMNet for the glaucoma detection framework is given in Figure 1.

In the proposed work, the various stages are (i) Image acquisition, (ii) Image enhancement, (iii) Abnormality segmentation, and (v) Hybrid classification. Here, the input images are gathered from the benchmark datasets. Here, the collected input images are given to the image enhancement phase to increase the image contrast, which is carried out through the multi-scale Retinex technique. Consequently, it helps to estimate the illuminance of images. Moreover, it offers better compression and total rendition of the dynamic range of all the images. It efficiently restores the color of an original image. Hence, the recommended model helps to increase the quality of images. Next, the Modified DeepLabV3 is implemented by adopting IROA for the segmentation process will be carried out to segment the abnormalities. Moreover, the parameters are optimized by DeepLabV3,

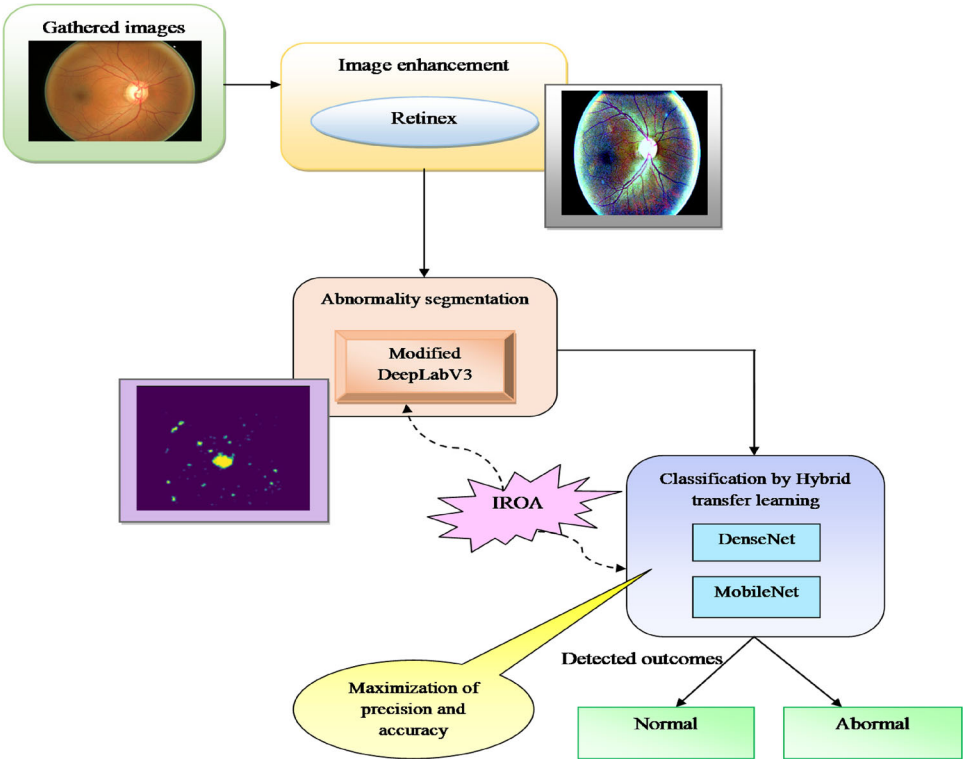

Figure 1. The architecture of the designed ODMNet for glaucoma detection framework using IROA.

which helps to increase the performance of glaucoma detection. This technique is more helpful in segmenting the objects at various scales to offer better segmentation of abnormalities. The efficient segmentation process helps to improve the detection rate of glaucoma detection (Shyamalee and Meedeniya 2022a; Venugopal et al. 2022b). Then, the segmented images are given to the detection or classification task, where the hybrid learning method with DenseNet and MobileNet approaches is utilized for effective classification, where the parameters of both DenseNet and MobileNet are optimized by the IROA algorithm. It helps to increase the efficiency of the recommended technique regarding the precision and accuracy of the glaucoma detection model. Transfer learning is more eminent as it saves resources and time without training various models. Thus, this approach is more suitable for performing glaucoma detection.

3.2. Description of Glaucoma Detection Dataset

In this proposed ODMNet-based glaucoma detection framework, the iris images are gathered in https://www.kaggle.com/datasets/sshikamaru/glaucoma-detection?select=glaucoma.csv (accessed August 26, 2022). Glaucoma can able to damage the optic nerve, which affects the vision of the eye.

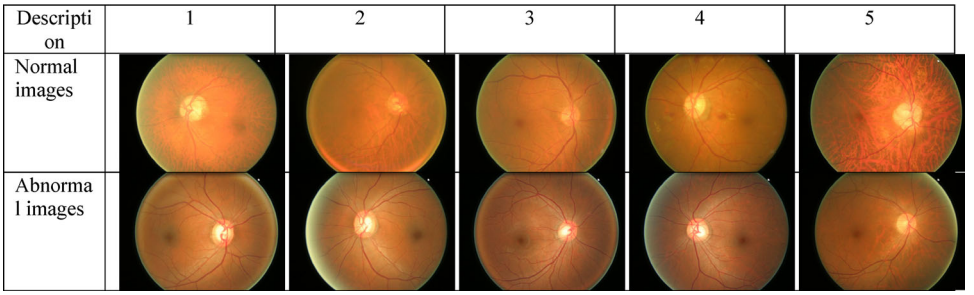

Figure 2. Sample images of all classes in the gathered dataset.

Moreover, the damage occurs due to high pressure in the eye. Hence, glaucoma is a common disorder at the age of 60. It comprises OCT Scans or images of the eye. It has two classes, normal and abnormal images of glaucoma disease. This dataset has a total of 650 images. Moreover, OCT scan images of the eye are taken to detect glaucoma. Some acquired sample images are listed in Figure 2. At last, the obtained images are known as Z_i, where $i = 1, 2, 3, \ldots, I$ and the entire gathered images are specified as I.

4. Image enhancement and optimized deeplabv3 for abnormality segmentation

4.1. Retinex-Based Image Enhancement

In this model, the standard Retinex-based image enhancement is carried out on the collected images Z_i.

As the eye includes the complicated nature of glaucoma lesions, including structure, color, and size differentiations, the processing and identification of glaucoma are complex. Thus, there is a need for a standard approach that is used to increase the image contrast. In this model, the multi-scale Retinex-based image enhancement increases the contrast. It performs nonlinear color conversion to get better and clear details of the images and also highlights the necessary information owing to various illumination conditions. Some images may have imbalanced illumination of background due to the lack of loss of details and quality of acquired images. The multi-scale Retinex-based image enhancement (Zotin 2018) is defined as a weighted sum of several Single-Scale Retinex outputs. It is more efficient in balancing the tradeoff between the color rendition and dynamic range compression. It is mathematically formulated in Eq. (1).

$$Z_i^{MSR}(a, b, \sigma) = \sum_{r=1}^{m} \omega (Z_i^{MSR})_r (a, b, \sigma_r) \tag{1}$$

In Eq. (1), the r^{th} component of the scale is specified as (Z_i^{MSR}), the vector of the blurring coefficients is mentioned as $\sigma = \{\sigma_1, \sigma_2, \ldots \sigma_r\}$, the

weight correlated with r^{th} scale is denoted as ω_r, where $\omega_1 + \omega_2 + \omega_3 + \cdots + \omega_m = 1$ and the number of scales is noted as m.

Finally, the color and lightness rendition derived images are attained by multi-scale Retinex that is known as Z_i^{MSR} and fed to the next stage.

4.2. Abnormality Segmentation by Optimized DeepLabv3 Model

The proposed glaucoma detection model recommends a new modified DeepLabv3 approach by optimizing the parameters in DeepLabv3 for performing the abnormality segmentation in contrast-enhanced images Z_i^{MSR} and efficiently segmenting the abnormalities in the images.

DeepLabv3 (Sreng et al. 2020) is the extended version of the DeepLabv2 model, which uses the pre-trained CNN model with VGG-16/ResNet-101 with atrous convolution for gathering the features from the images. The usage of atrous convolution in DeepLabv3 helps in producing fine-segmented outcomes with the use of the conditional random field, conversion of images into a dense feature extractor without the need for learning parameters, and better monitoring of resolution in feature outcomes. It has the advantage of using an Atrous Spatial Pyramid Pooling (ASPP) module with image-level features. Then, the batch normalization technique is performed in DeepLabv3 to train the network. The approach performs by initializing with batch normalization, a 1×1 convolution, and a ReLU, and this result is given into the ASPP. The convolution operations in the pyramid are 3×3 with different dilation rates, which uses the adaptive average pooling for global context and four convolution operations with batch normalization and ReLU activation steps.

This technique extends the field of view of filters for incorporating the huge context and helps control the resolution of acquired features. The multi-scale context is attained by using the ASPP with diverse atrous rates. The DeepLabV3 achieves higher performance by the usage of ASPP that comprises diverse rates of four parallel atrous convolutions given to the feature map. Next, batch normalization is carried out after pyramiding the atrous convolutions. Then, the global average pooling is applied for the feature map in the network via global context that is further followed by batch normalization and 1×1 convolution. At last, the bi-linear upsampling is performed to get the results in the specified dimension. ResNet101 is utilized as the backbone of this DeepLabV3 network. Here, to further enhance the efficiency of the designed segmentation framework, the learning rate and epochs in Deeplabv3 are optimized using the IROA algorithm. Here, the optimal parameter tuning helps maximize the abnormality segmentation accuracy rate on the proposed model. The primary objective of the designed abnormality segmentation using IROA-based Deep Labv3 is

derived in Eq. (2).

$$F_1 = \arg\min_{\{ep, lr\}} \left(\frac{1}{cy}\right) \tag{2}$$

Here, the learning rate and epochs in Deeplabv3 are accordingly known as lr and ep, are optimized using the IROA algorithm, where the epochs in Deeplabv3 are assigned in the range of [50, 100], and the learning rate in Deeplabv3 is allocated in the limit of [0.01, 0.99]. Next, accuracy is specified as cy the ratio of the observation of exactly predicted to the whole observations.

$$cy = \frac{(PT + NT)}{(PT + NT + PF + NF)} \tag{3}$$

Here, variables PT, NT, PF, and NF. refer to the true positives, true negatives, false positives, and false negatives, respectively. Finally, the segmented abnormality images using the optimized DeepLabv3 model are specified $Z_i^{\text{DeepLabv3}}$.

The architecture framework of the proposed optimized DeepLabv3 model for abnormality segmentation using IROA is depicted in Figure 3.

4.3. Proposed IROA

In the recommended glaucoma detection and classification model, a new meta-heuristic strategy is implemented to maximize the performance of the detection rate. It is designed for better segmentation and detection efficiency, where the epochs and learning rate in DeepLabV3 is optimized for better abnormality segmentation, and the epochs in DenseNet and MobileNet are optimized for precise detection of glaucoma. This parameter tuning helps in maximizing the efficiency rate of the glaucoma detection and classification model. This heuristic improvement is derived for maximizing the detection rate for assisting ophthalmologists in treating patients in preventing permanent vision loss.

ROA (Moazzeni and Khamehchi 2020) is selected due to its efficient and simpler searching operation, which can offer optimal solutions at huge searching dimensions with a lower time. However, it further requires convergence rate improvement. In this paper, a new fitness-derived formula is adopted for the volume of a droplet χ, which results in a superior performance of detection rate.

ROA is formulated by observing the nature of rainfall. While starting the rainfall, the droplets are felt on the earth's surface. Next, the combination of droplets is done with one another, and it is merged. Some droplets must be noticed or exhaust the soil with the soil features such as wettability,

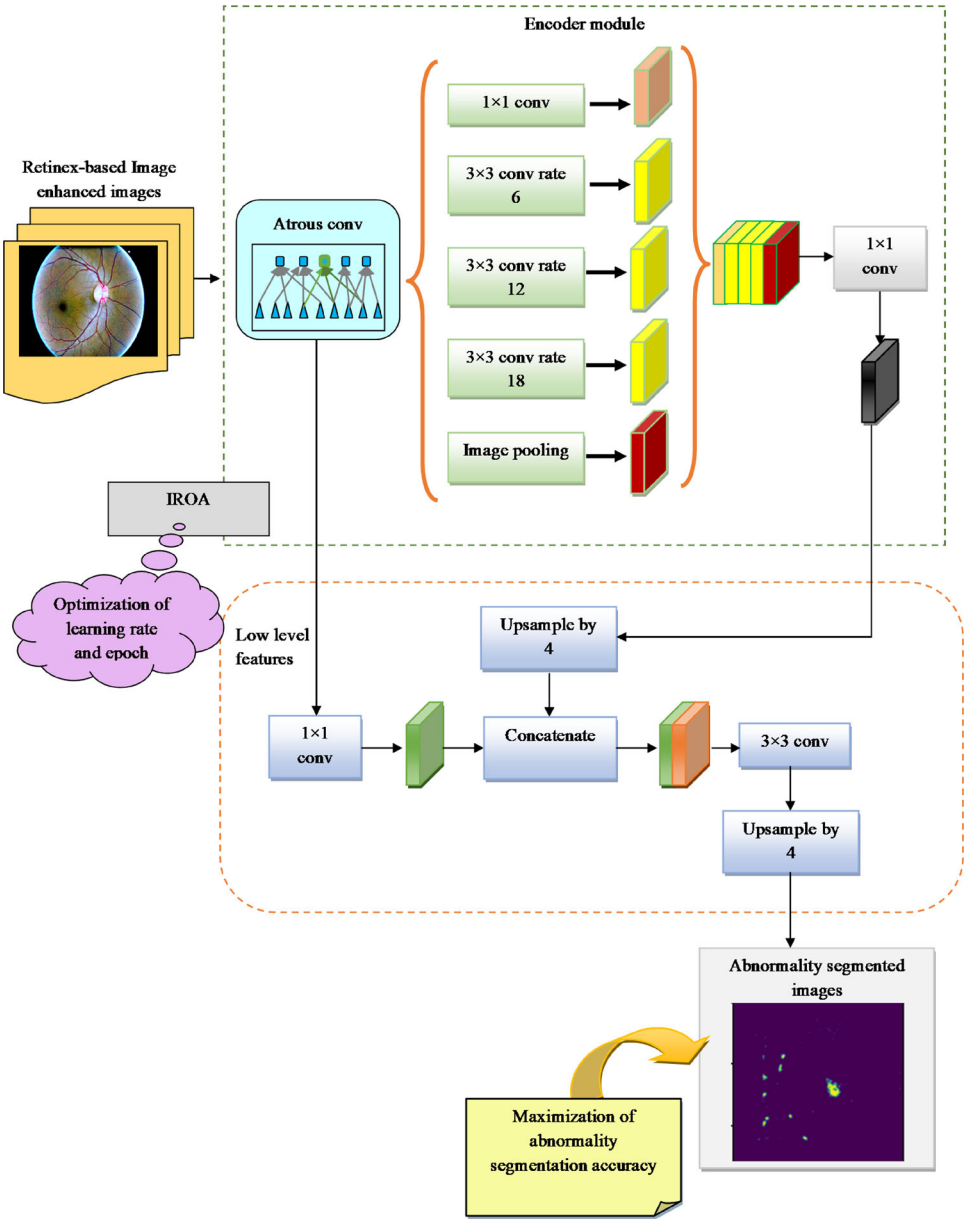

Figure 3. Optimized Deep Labv3 Model for abnormality segmentation using IROA.

permeability, porosity, the texture of the soil surface, etc. Water dissolved some soil and vanished from the environment. The water can be further fed into the river or other water sources. ROA is formulated based on the type of rainfall, including high, medium, and lower rainfall. Thus, ROA formulates a set of solutions based on the movement of water from the best solution to the worst solution. A raindrop is referred to as each solution in the environment. However, the random search space is considered

due to the huge area of the surface. The main feature of a drop of rain is the radius, which is restricted as time passes and is known as raindrops that are correlated with other drops. While generating the initial population, the allocation of the radius of each droplet is done arbitrarily for a certain limit. In addition, the neighborhood is validated by every droplet by taking the size. Moreover, every droplet is included with $d-$ variables for solving the problems in the dimensional area. Initially, the minimum and maximum range of the variable is evaluated as the limits that are designed with a radius of the droplet.

Then, the sampling of two endpoints of the variable is done, and it is carried out until getting the final variable. Then, it upgrades the cost of the initial droplet by forwarding in a downward direction. It is applied for every droplet, and the allocation of position and cost of each droplet is done. Two ways are used for modifying and determining the radius of a droplet, as shown here. Radius is estimated by measuring the two droplets with radius rd_1 and rd_2, by taking the radius, one droplet is closer to the other droplet, and it links to develop a huge droplet of radius Rd as estimated in Eq. (4).

$$Rd = (rd_1^d + rd_2^d)^{\frac{1}{d}} \tag{4}$$

Here, the number of variables for entire droplets is known as d. If a droplet with a radius rd_1 is not shifted, it takes the soil features that are noticed by term χ as derived in Eq. (5), and then the water is noticed by the soil.

$$Rd = (\chi \cdot rd_1^d)^{\frac{1}{d}} \tag{5}$$

In Eq. (5), the volume of a droplet is specified χ, which is described based on the minimum and maximum radius of droplets as shown in conventional ROA. While in the proposed IROA, the droplet volume χ.is updated via the formulation of best and worst fitness solutions as equated in Eq. (6).

$$\chi = \frac{F_{best}}{F_{worst}} \tag{6}$$

Here, the worst solution is derived F_{worst}, and the best solution is termed F_{best}. Next, the diameter of droplets plays a significant role in maximizing the local searching of drops, and it enhances the analysis process. Hence, weaker droplets will be avoided or linked with reliable drops by increasing the maximum number of rounds, where the initial population is intensively minimized.

The pseudocode of the designed IROA is depicted in Algorithm 1.

Algorithm 1: Recommended IROA

Input: learning rate *lr* and epochs *ep* of Deeplabv3;
epochs of DenseNet *es*, epochs of MobileNet *em*
Output: Optimal solution
The population is initiated randomly
Determine the random parameters
Determine the position, size, and radius of droplets
Estimate every droplet with the fitness function to get the cost of every droplet
Sorting the population via a fitness function
  While (iteration < maximum number of iterations)
    For every droplet
      Evaluate each solution and update the new location of droplets
      Accept new solution while new fitness function is lower than the earlier one
      While (lower fitness is noticed)
        Update the number of variables using Eq. (5)
        Update the volume of the droplet by Eq. (6)
        Evaluate the radius of droplets using Eq. (4)
        Link the droplets by considering the radius is closer to other droplet
      End while
    End for
  End while
End
Achieve optimal solutions
Terminate

The processing steps of the proposed IROA are given here. Formulate the population randomly, where the modification is done in the initial population number after entire iterations owing to the relation with neighboring drops. It increases searchability and minimizes the cost of optimization (Nath and Dandapat 2012; Kar et al. 2022). If the size of one droplet is modified, then the nearer droplets will be linked or absorbed by the soil. It increases the searching ability of each droplet, and droplets are classified. Here, the droplet volume is updated via the best and worst fitness solutions. Finally, the optimal solutions are updated by considering the fitness-based solutions. A flowchart of the proposed IROA for the designed glaucoma detection and classification model is given in Figure 4.

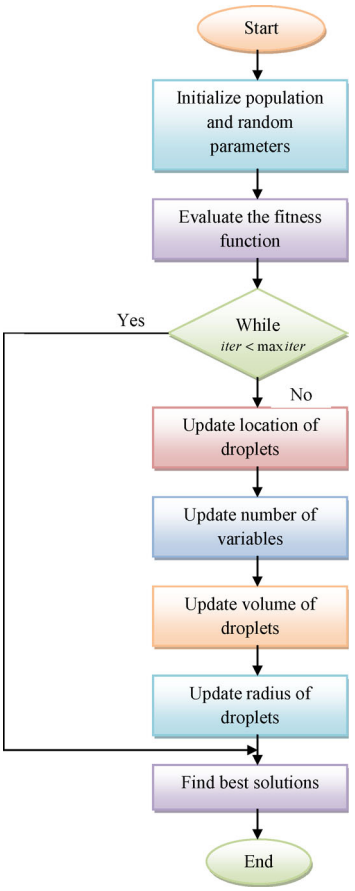

Figure 4. Flowchart of proposed IROA for the designed glaucoma detection and classification model.

5. Modified DenseNet and MobileNet with Architecture Optimization for Glaucoma Detection and Classification

5.1. Basic DenseNet

In the recommended glaucoma detection and classification model, the DenseNet (Sudhan et al. 2022) is used. DenseNet is a complicated CNN that utilizes a dense framework for linking entire layers in an efficient manner that results in dense intercorrelations among layers. Every layer gets additional inputs from entire prior levels and is forwarded to its feature maps for maintaining the feed-forward nature. The DenseNet is the advanced form of ResNet. Some of the advantages of DenseNet are shown here. In DenseNet, it helps to reduce the number of parameters, avoids feature repetition, enhances feature propagation, and solves vanishing gradient issues. The DenseNet offers significant performance over other traditional approaches that achieve superior outcomes and reduce computational complexity.

DenseNet uses ResNets for performing nonlinear transformation of input images as abnormality-segmented images using an optimized DeepLabv3 model $Z_i^{\text{DeepLabv3}}$ via a skip connection, as shown in Eq. (7).

$$z_\ell = Hf_\ell(z_{\ell-1}) + z_{\ell-1} \tag{7}$$

Here, the output of ℓ^{th} the layer is mentioned as z_ℓ a composite function of operations is denoted as $Hf_\ell(\cdot)$. ResNets perform the direction flow via the identity function from the previous layers to the former layers. The information flow can be directed in the network using the summation of the result Hf_ℓ. The next process is dense connectivity, which carries out the direct connections from any layer to other layers. The feature maps of previous layers are received by ℓ^{th} layer. Different inputs $Hf_\ell(\cdot)$ are concatenated for simpler implementation.

Then, DenseNets comprises pooling layers, which perform the concatenation operation while changing the size of the feature maps. The network is further categorized into various densely connected dense blocks for facilitating down-sampling in this architecture. The transition layers are used here with the combination of pooling and convolution layers, which include a 2×2 average pooling layer, 1×1 convolutional layer, and batch normalization layer. The growth rate is taken as one of the hyper-parameters of the network. The next layer is the bottleneck layer, which generates the output feature maps with several inputs. It minimizes the number of input feature maps. It helps to enhance the computational efficiency and minimize the number of input feature maps. Then, the compression operation reduces the number of input feature maps at transition layers.

At last, this network retrieves the output as normal and abnormal classes for the designed glaucoma detection and classification model. The general framework of DenseNet architecture for glaucoma detection and classification is given in Figure 5.

5.2. Basic MobileNet

In the recommended glaucoma detection and classification model, the MobileNet (Elangovan and Nath 2022) is used for classification purposes. It takes the input as abnormality-segmented images using an optimized DeepLabv3 model $Z_i^{\text{DeepLabv3}}$. Moreover, the MobileNet is utilized for detecting glaucoma disease. Hence, the MobileNet is lightweight architecture to classify the detected glaucoma. Additionally, it helps to filter the channels more effectively. Consequently, it achieves low maintenance costs and performs well with high speed.

MobileNet is a recent transfer learning approach broadly utilized in various applications. It is generally built from CNN architecture with a

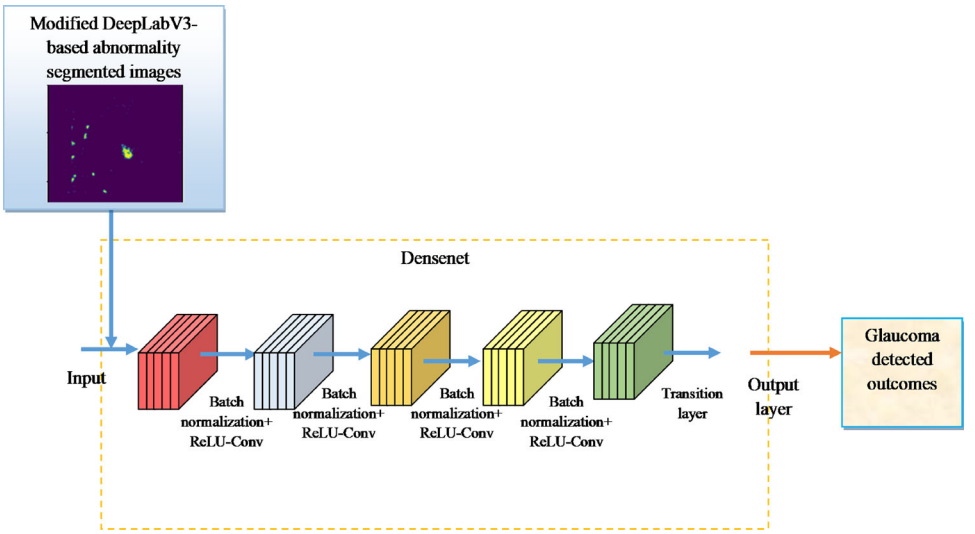

Figure 5. DenseNet architecture for glaucoma detection and classification model.

minimized number of constraints. It results in higher detection accuracy in existing studies. It is designed with the integration of 3×3 downsampling convolutional layers for getting the features and uses the average pooling layer before utilizing the fully classified layers. It is further included with pointwise and depth-wise convolutions for performing the depth-wise separable convolutions to minimize the number of parameters. It initially aims to divide the spatial dimension and depth of the filter. Thus, this network is more suitable for medical image classification tasks.

Initially, the abnormality-segmented images using the optimized DeepLabv3 model $Z_i^{\text{DeepLabv3}}$ is divided into feature map Fe fed into the convolution layer and attain the outcomes Ot, in which the attained feature map Fm is processed via the spatial height and width of the squared results. It is modeled in Eq. (8).

$$Ot_{e,f,g} = \sum_{p,q,s} K_{p,q,s,g} \cdot Fe_{e+p-1,f+q-1,s} \tag{8}$$

Here, the number of output channels is given as Gs, and the number of input channels is indicated as Fe, kernel size is denoted as K. Depthwise separable convolutions is used in this network for breaking the associations among the kernel size and the number of resultant channels, where the filtering of features is performed along with the regular convolution operation via the convolutional kernels. The two layers of depthwise separable convolution are depthwise convolutions and pointwise convolutions. Moreover, a single input depth or channel is applied in depthwise convolutions. Then, a linear integration of the output is created by using pointwise convolution. In such layers, the ReLU and batch norm are utilized. Next,

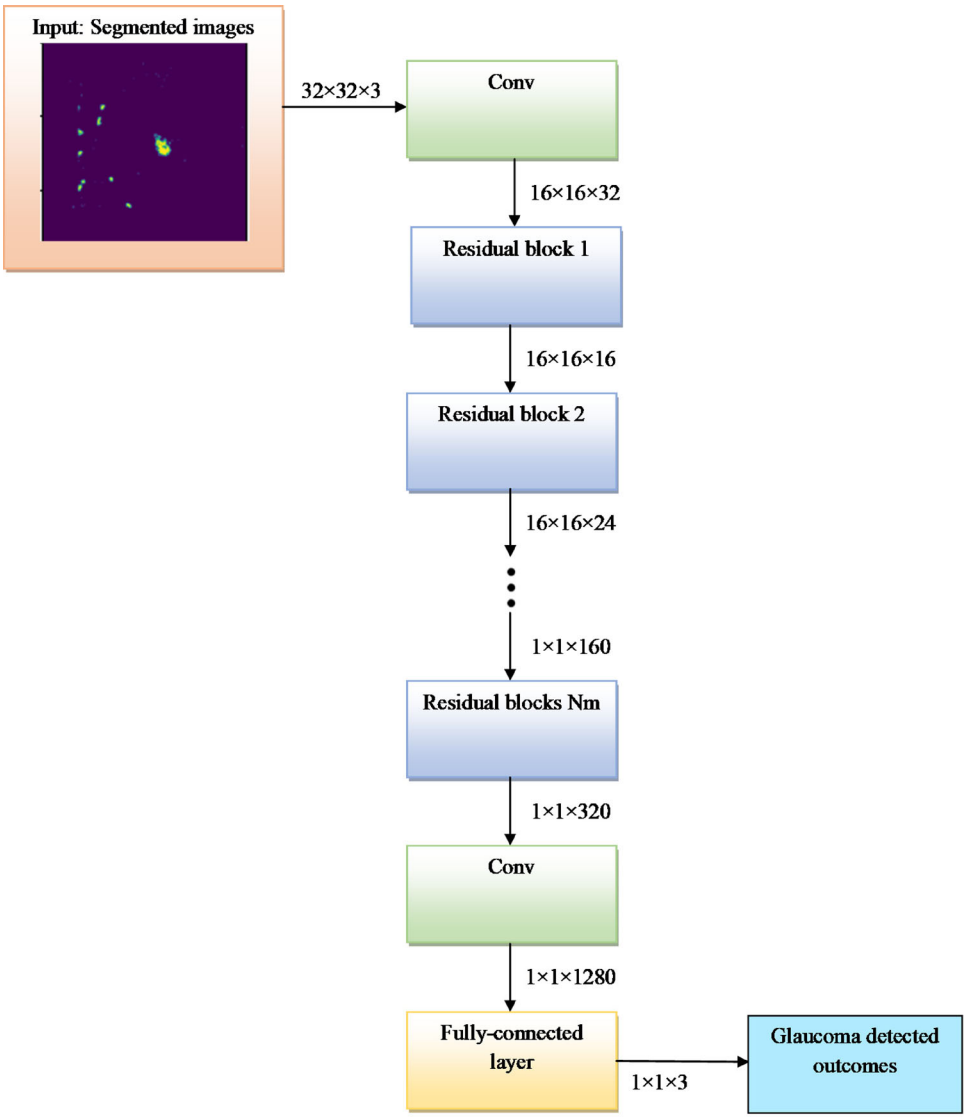

Figure 6. MobileNet architecture for glaucoma detection and classification.

3×3 depthwise separable convolutions rather than regular convolutions are suggested for performance enhancement. Then, the final average pooling is taken for reducing the spatial resolution to 1 before utilizing the fully connected layer.

Finally, this network retrieves the output as normal and abnormal classes for the designed glaucoma detection and classification model. The general framework of MobileNet architecture for glaucoma detection and classification is depicted in Figure 6.

5.3. Proposed ODMNet

In the designed glaucoma detection and classification model, new ODMNet is designed for precise detection of glaucoma and classified the outcomes of both MobileNet and DenseNet into normal and abnormal classes, where the input of both MobileNet and DenseNet is taken as the abnormality segmented images using optimized DeepLabv3 $Z_i^{\text{DeepLabv3}}$. The ODMNet is designed by taking the averaging among outcomes of MobileNet, and DenseNet, and results are attained precisely to ensure the precision and accuracy maximization of the glaucoma detection rate. As a major contribution, a new optimized MobileNet and optimized DenseNet are designed with the adoption of IROA, where the Epochs in DenseNet and MobileNet for enhancing the superiority of the glaucoma detection and classification model via ODMNet. This contribution is adopted for enhancing performance and also helps in contributing to the medical field.

MobileNet is chosen here owing to its features like lower computation and higher computational efficiency. It has managed the downsampling with strided convolution in the first layer and depthwise convolutions. Similarly, DenseNet is selected in this architecture for its vast features like considerable reduction in the number of parameters, avoiding feature repetition, enhanced feature propagation, and solving vanishing gradient issues. The DenseNet offers significant gains over other traditional approaches that achieve superior performance and reduce computational complexity. Thus, the combination of both MobileNet and DenseNet helped in maximizing the performance of the glaucoma detection and classification model. The major goal of the ODMNet-based glaucoma detection and classification model is taken as the maximization of accuracy and precision rates. It is mathematically derived in Eq. (9).

$$F_2 = \underset{\{es,\, em\}}{\arg\min} \left(\frac{1}{cy + prc} \right) \tag{9}$$

Here, the Epochs in DenseNet and MobileNet are correspondingly termed as *es* and *em*, respectively, which is optimized and assigned in the range of [50, 100] using IROA. The precision is known as *prc* and is described as the ratio of positive observations that are predicted exactly to the total number of observations that are positively predicted, as equated in Eq. (10).

$$prc = \frac{PT}{PT + PF} \tag{10}$$

Thus, finally, the designed model considerably aims to maximize the performance and result in superior efficiency, which is proved in the result section. A new ODMNet framework for glaucoma detection and classification model is depicted in Figure 7.

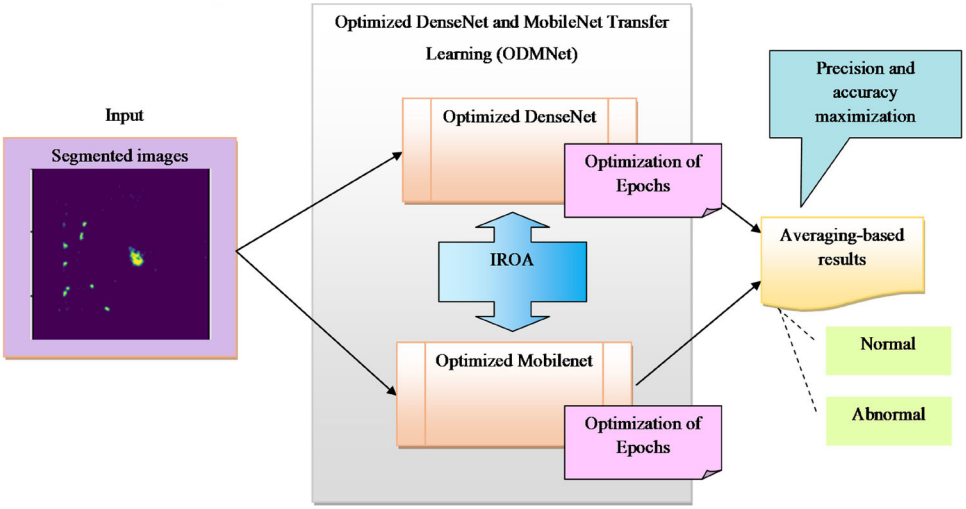

Figure 7. ODMNet framework for glaucoma detection and classification model using IROA.

6. Result Evaluation

6.1. Experimental Settings

The suggested glaucoma detection and classification model was experimented in Python. Here, Type I measures were positive measures like Accuracy, Sensitivity, Specificity, Precision, Negative Predictive Value (NPV), F1Score, Mathews correlation coefficient (MCC), and Type II measures were negative measures like False positive rate (FPR), False negative rate (FNR), and False Discovery Rate (FDR). It was measured using various traditional approaches like CNN (Patel and Singh 2021), DenseNet (Sudhan et al. 2022), MobileNet (Elangovan and Nath 2022), Ensemble (Nayak et al. 2021), and heuristic techniques like Particle Swarm Optimization (PSO) (Pedersen and Chipperfield 2010), Grey Wolf Optimizer (GWO) (Mirjalili, Mirjalili, and Lewis 2014), Coyote Optimization algorithm (COA) (Mirjalili, Mirjalili, and Lewis 2014), and ROA (Moazzeni and Khamehchi 2020). The experimental analysis was done by taking the parameters such as number of populations as 10, chromosome length as 2, and maximum iteration as 10.

6.2. Performance Measures

Diverse performance metrics are estimated for evaluating the performance, and it's described below.

(a) F1 score: harmonic mean between precision and recall. It is used as a statistical measure to rate performance.

$$F1score = \frac{2PT}{2PT + PF + PN} \tag{11}$$

MCC: correlation coefficient computed by four values.

$$MCC = \frac{PT \times NT - PF \times NF}{\sqrt{(PT + FP)(PT + FN)(NT + PF)(NT + NF)}} \tag{12}$$

NPV: the probability that subjects with a negative screening test truly don't have the disease.

$$NPV = \frac{NT}{NT + FN} \tag{13}$$

FDR: the number of false positives in all rejected hypotheses.

$$FDR = \frac{FP}{FP + PT} \tag{14}$$

FPR: the ratio of the count of false positive predictions to the entire count of negative predictions.

$$FPR = \frac{PF}{PF + NT} \tag{15}$$

FNR: the proportion of positives which yield negative test outcomes with the test.

$$FNR = \frac{NF}{NT + PT} \tag{16}$$

Sensitivity: the number of true positives, which are recognized exactly.

$$Se = \frac{PT}{PT + NF} \tag{17}$$

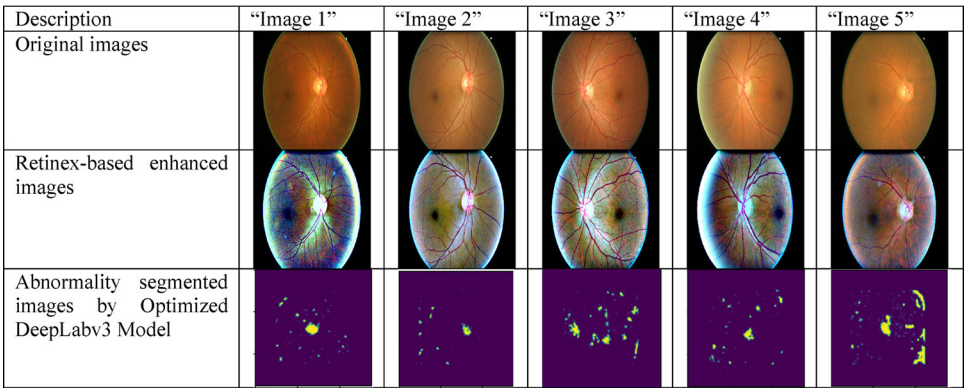

Figure 8. Sample experimental outcomes of the designed glaucoma detection and classification.

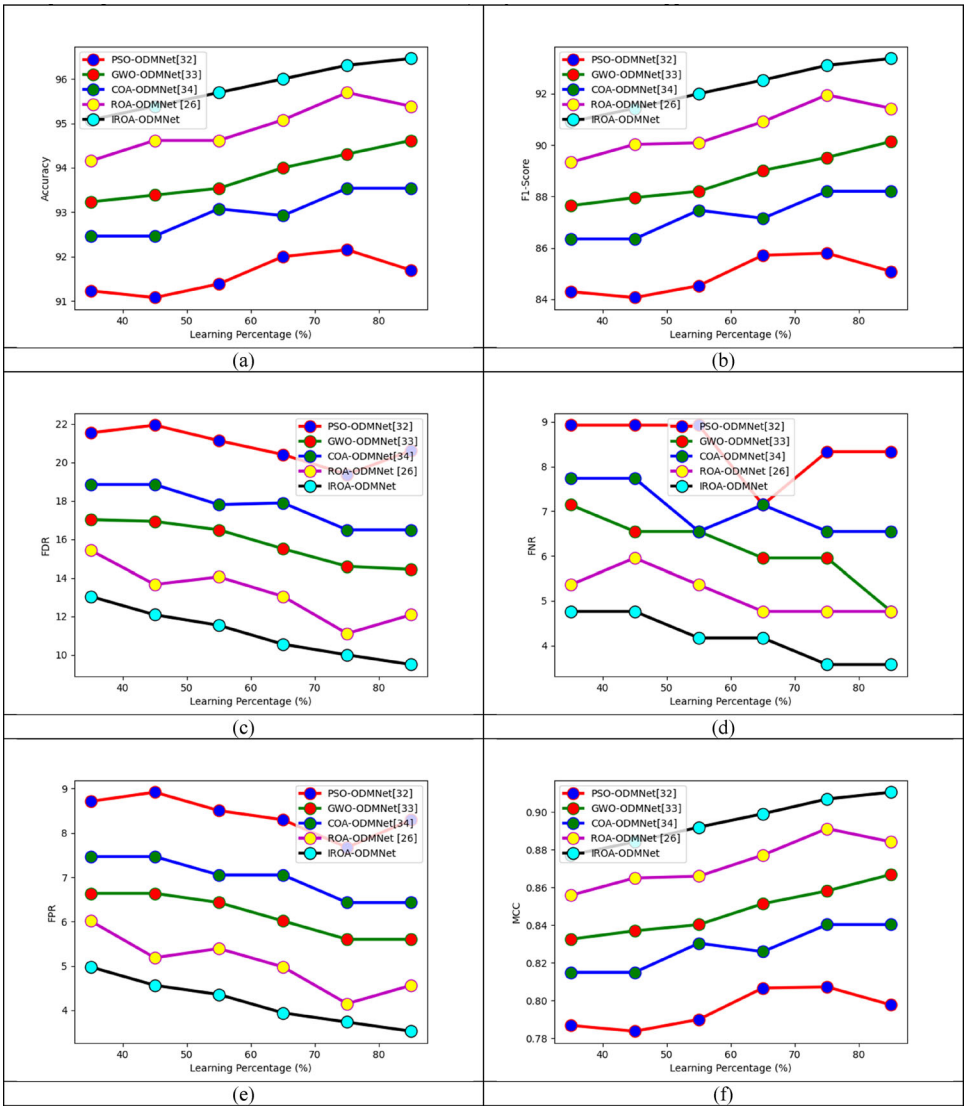

Figure 9. Result interpretation on the designed glaucoma detection and classification model over heuristic techniques regarding (a) Accuracy, (b) F1-score, (c) FDR, (d) FNR, (e) FPR, (f) MCC, (g) NPV, (h) Precision, (i) Sensitivity and (j) Specificity.

Specificity: the number of true negatives, which are determined precisely.

$$Sp = \frac{NT}{NT + PF} \tag{18}$$

6.3. Experimental Outcomes

This section gives the experimental outcomes of the designed glaucoma detection and classification model with the considered processing steps, which are depicted in Figure 8.

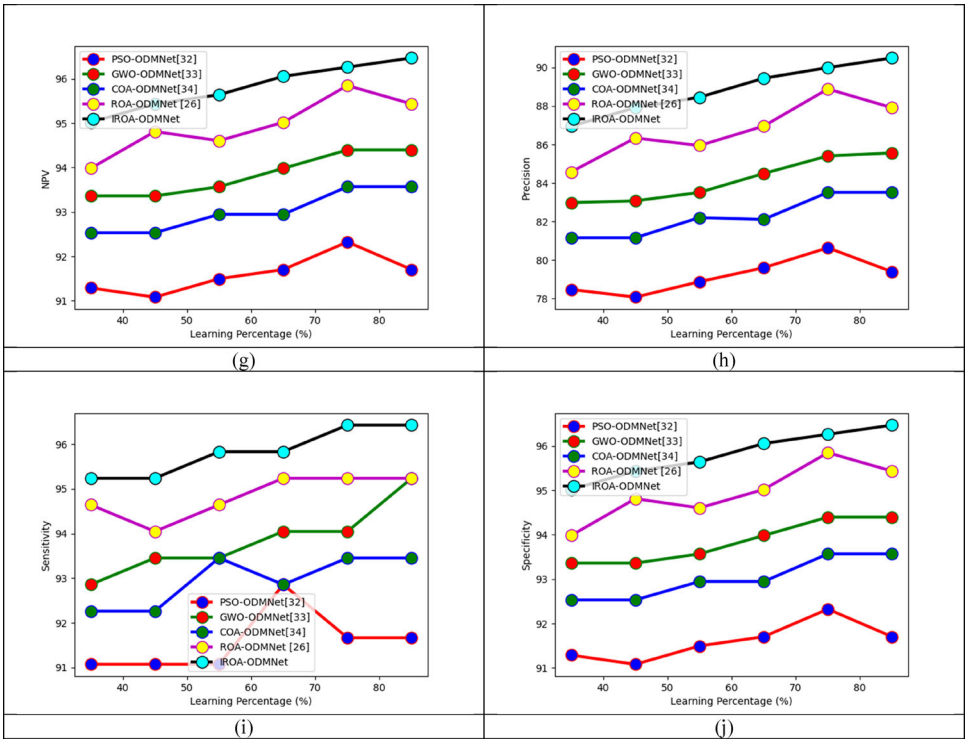

Figure 9. Continued

6.4. Result Interpretation over Heuristic Techniques

Figure 9 illustrates the performance estimation of recommended glaucoma detection and classification model by estimating with diverse optimization algorithms. The recommended IROA-ODMNet with abnormality segmentation by optimized DeepLabv3 model exhibits higher efficiency than other techniques. The F1-score of the implemented IROA-ODMNet is 10.3%, 4.2%, 6.5%, and 0.8% progressed than PSO-ODMNet, GWO-ODMNet, COA-ODMNet, and ROA-ODMNet techniques at 85%. The graph analysis shows the equivalence performance. Moreover, the F1-score of the ROA algorithm has shown a second better performance at the learning percentage of 60. Hence, the PSO algorithm has attained a high error rate which leads to degrade the system performance. However, the overfitting issues were not resolved by the PSO algorithm. Thus, the simulation analysis of the suggested glaucoma detection and classification model using IROA-ODMNet exhibits superior performance in terms of detection rate in analyzing the conventional approaches.

6.5. Result Interpretation over Transfer Learning Techniques

The result evaluation on the designed glaucoma detection and classification model over traditional learning methods is depicted in Figure 10.

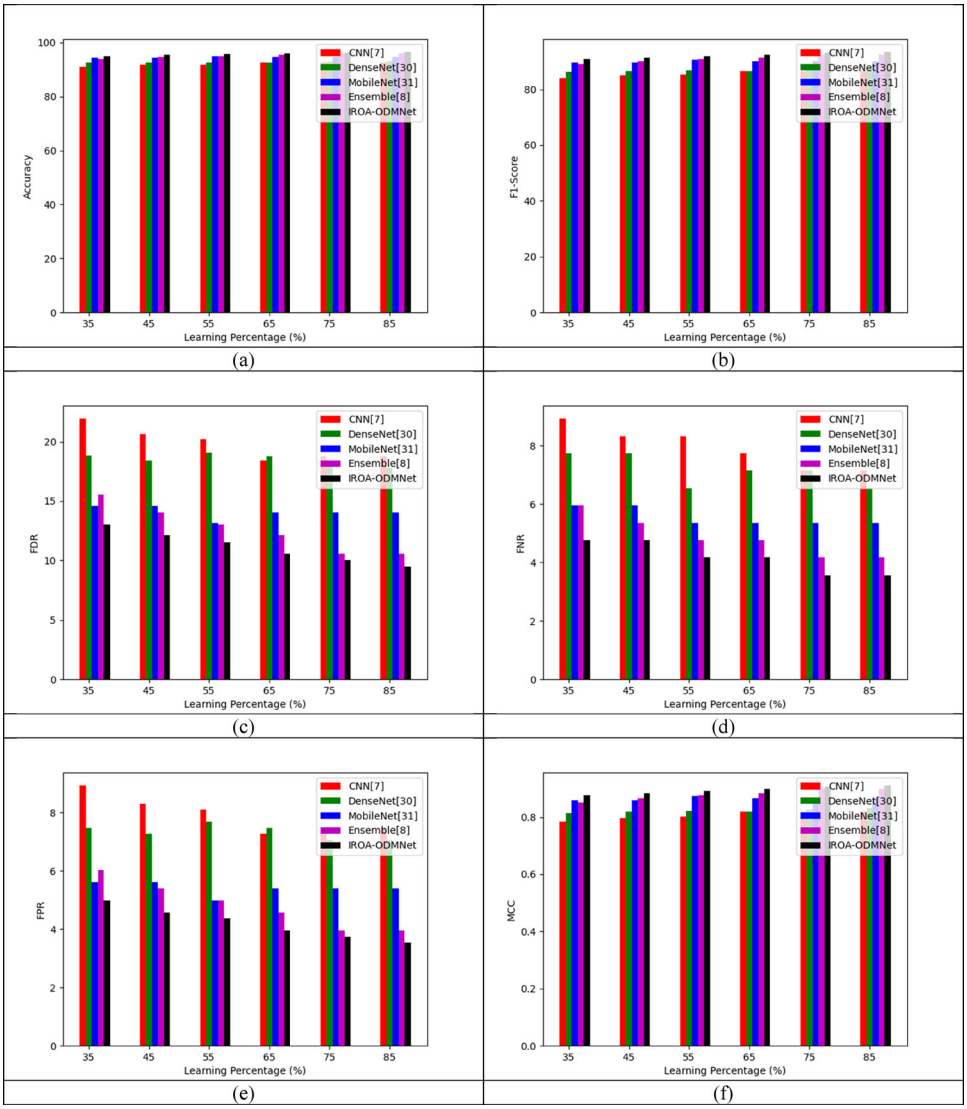

Figure 10. Result interpretation on the designed glaucoma detection and classification model over existing techniques regarding (a) Accuracy, (b) F1-score, (c) FDR, (d) FNR, (e) FPR, (f) MCC, (g) NPV, (h) Precision, (i) Sensitivity and (j) Specificity.

The estimation on IROA-ODMNet exhibits higher performance values and results in superior efficiency on detection. The evaluation is done by varying the learning percentages and achieving higher efficiency in terms of both positive and negative measures. This analysis with IROA-ODMNet has achieved better efficacy, in which the MCC of the suggested IROA-ODMNet is correspondingly 13.9%, 13.9%, 7%, and 4% higher than CNN, DenseNet, MobileNet, and Ensemble techniques at 55%. Here, the Ensemble model attains a second better performance regarding the F1-score. Additionally, CNN has a higher error rate, affecting system

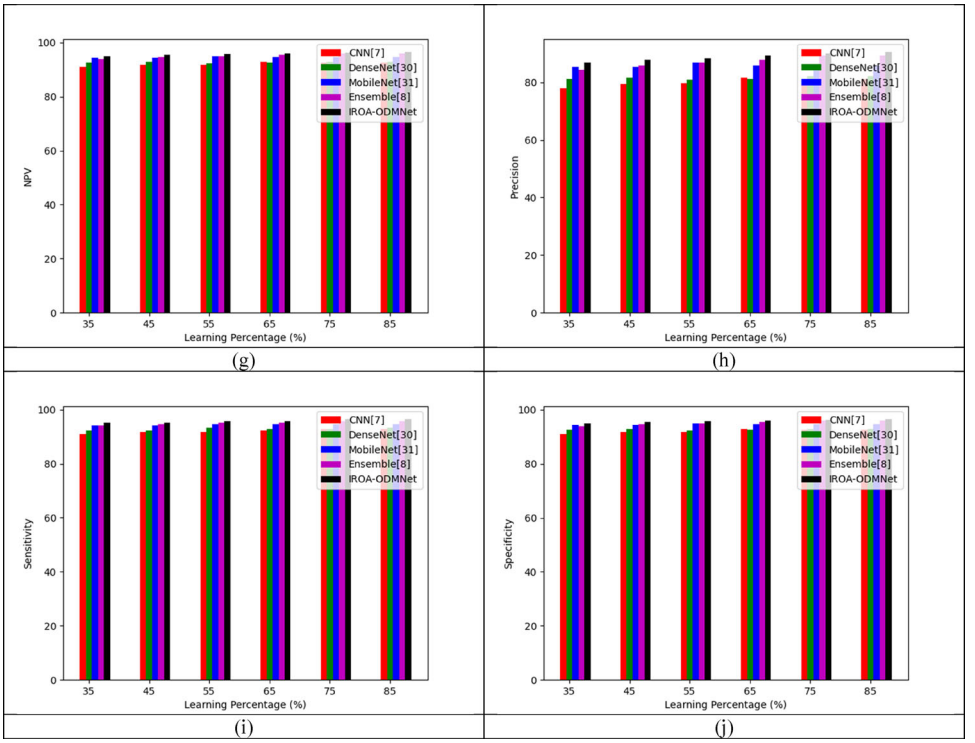

Figure 10. Continued

Table 2. Result interpretation of the designed glaucoma detection and classification model over heuristic techniques.

Measures	PSO-ODMNet (Pedersen and Chipperfield 2010)	GWO-ODMNet (Mirjalili, Mirjalili, and Lewis 2014)	COA-ODMNet (Yuan et al. 2020)	ROA-ODMNet (Moazzeni and Khamehchi 2020)	IROA-ODMNet
Accuracy	92.15385	94.30769	93.53846	95.69231	96.30769
Sensitivity	91.66667	94.04762	93.45238	95.2381	96.42857
Specificity	92.32365	94.39834	93.56846	95.85062	96.26556
Precision	80.62827	85.40541	83.51064	88.88889	90
FPR	7.676349	5.60166	6.431535	4.149378	3.73444
FNR	8.333333	5.952381	6.547619	4.761905	3.571429
NPV	92.32365	94.39834	93.56846	95.85062	96.26556
FDR	19.37173	14.59459	16.48936	11.11111	10
F1-Score	85.79387	89.51841	88.20225	91.95402	93.10345
MCC	0.807206	0.858112	0.840237	0.891164	0.90687

performance. Evaluating the suggested glaucoma detection and classification model using IROA-ODMNet exhibits superior over other approaches.

6.6. Comparative Study

The estimation of the glaucoma detection and classification model is analyzed with both heuristic and traditional approaches, as shown in Tables 2 and 3. This analysis depicts that the designed IROA-ODMNet model gets

Table 3. Result interpretation of the designed glaucoma detection and classification model over learning techniques.

Measures	CNN (Patel and Singh 2021)	DenseNet (Sudhan et al. 2022)	MobileNet (Elangovan and Nath 2022)	Ensemble (Nayak et al. 2021)	IROA-ODMNet
Accuracy	92.61538	92.92308	94.61538	96	96.30769
Sensitivity	92.85714	92.85714	94.64286	95.83333	96.42857
Specificity	92.53112	92.94606	94.60581	96.05809	96.26556
Precision	81.25	82.10526	85.94595	89.44444	90
FPR	7.46888	7.053942	5.394191	3.941909	3.73444
FNR	7.142857	7.142857	5.357143	4.166667	3.571429
NPV	92.53112	92.94606	94.60581	96.05809	96.26556
FDR	18.75	17.89474	14.05405	10.55556	10
F1-Score	86.66667	87.15084	90.08499	92.52874	93.10345
MCC	0.819394	0.825897	0.8659	0.899017	0.90687

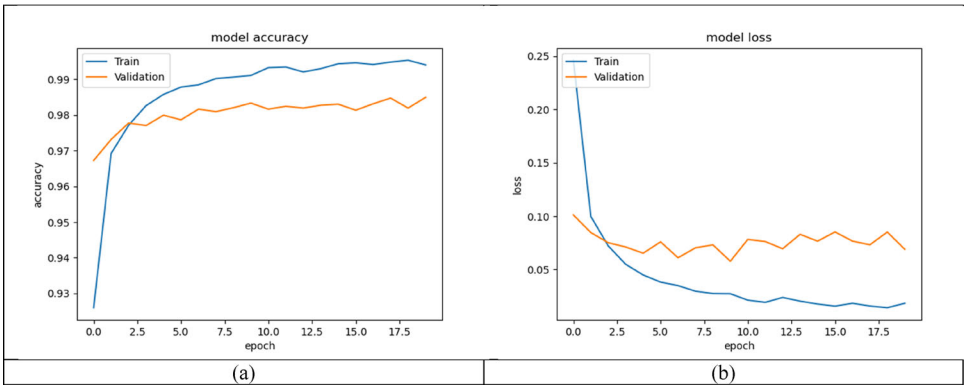

Figure 11. Evaluation of learning curves on the suggested model for glaucoma detection concerning (a) validation accuracy and (b) validation loss.

higher performance. The accuracy of the designed IROA-ODMNet is 4.5%, 2%, 2.9%, and 0.6% higher than PSO-ODMNet, GWO-ODMNet, COA-ODMNet, and ROA-ODMNet techniques. While considering the negative measures, the FPR of the recommended IROA-ODMNet is correspondingly 50%, 47%, 30%, and 5%, superior to CNN, DenseNet, MobileNet, and Ensemble techniques. Hence, the recommended approach has illustrated the higher efficiency in the proposed model.

6.7. Validation of Learning Curves on the Designed Model for Glaucoma Detection

Validation of learning curves on the designed IROA-ODMNet-based glaucoma detection method regarding accuracy is given in Figure 11.

6.8. Confusion Matrices of the Designed Glaucoma Detection Model

The confusion matrices on the developed glaucoma detection model are shown in Figure 12. Moreover, the graph analysis shows the predicted value of the recommended method is similar to the actual value.

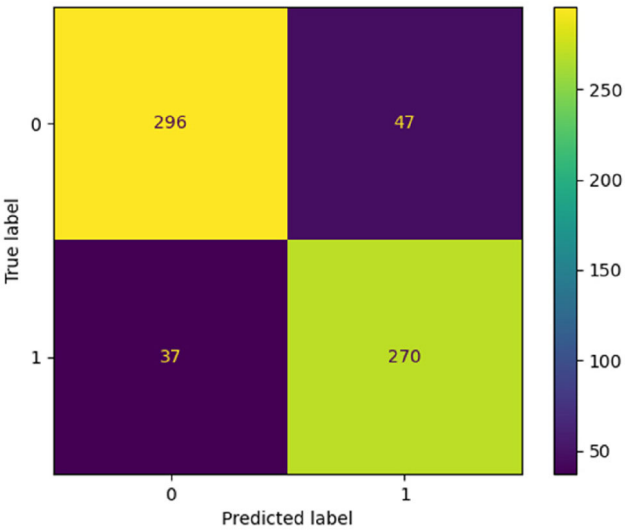

Figure 12. Confusion matrices of glaucoma detection model based on the true label.

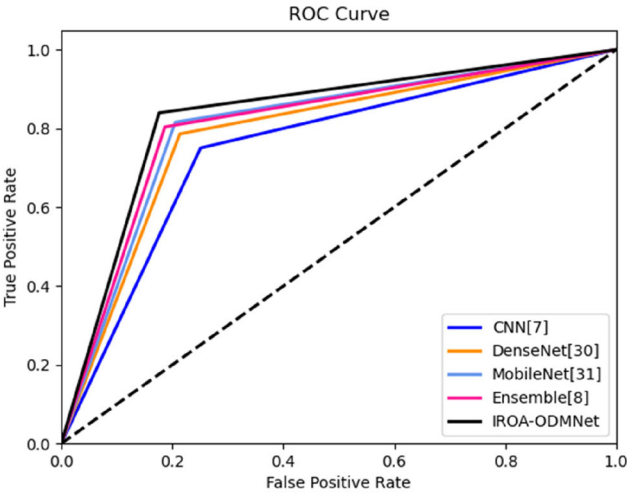

Figure 13. Validation of the ROC curve of the designed method.

6.9. ROC Curve for the Recommended Method for Detecting the Glaucoma

The ROC curve of the suggested IROA-ODMNet method of the glaucoma detection model is shown in Figure 13.

7. Conclusion

A new framework for glaucoma detection and classification model using a transfer learning approach was designed here. The digital fundus images were acquired from the standard datasets. These images were fed into the

Retinex approach for performing the image enhancement concept. Next, the segmentation process by Modified DeepLabV3 was designed in this approach, where the abnormalities were segmented along with IROA. This optimal parameter tuning in the suggested model has enhanced the accuracy of glaucoma detection. After segmenting the abnormalities in the images, they were fed into the detection or classification task performed via ODMNet. Here, the parameters in DenseNet and MobileNet were optimized using the same IROA algorithm. At last, the designed model was shown higher effectiveness with the assistance of diverse metrics. Here, the precision of the designed IROA-ODMNet was correspondingly 10%, 9.6%, 4.7%, and 0.6% maximized than CNN, DenseNet, MobileNet, and Ensemble techniques. Consequently, the designed model has illustrated the higher performance in terms of getting higher rates in positive measures and lower rates in negative measures, which has finally shown the superiority over others. However, this model has only been evaluated on small and standard datasets, which will be explored in the future by adopting large-scale and real-time datasets. The clinical practices will be performed in the future.

References

Abdullah, F., R. Imtiaz, H. A. Madni, H. A. Khan, T. M. Khan, M. A. U. Khan, and S. S. Naqvi. 2021. A review on glaucoma disease detection using computerized techniques. *IEEE Access*. 9:37311–33. doi:10.1109/ACCESS.2021.3061451.

Acharya, U. R., S. Dua, X. Du, V. Sree S, and C. K. Chua. 2011. Automated diagnosis of glaucoma using texture and higher order spectra features. *IEEE Transactions on Information Technology in Biomedicine* 15 (3):449–55. doi:10.1109/TITB.2011.2119322.

Afolabi, O. J., G. P. Mabuza-Hocquet, F. V. Nelwamondo, and B. S. Paul. 2021. The use of U-Net lite and extreme gradient boost (XGB) for glaucoma detection. *IEEE Access* 9: 47411–24. doi:10.1109/ACCESS.2021.3068204.

Alghamdi, M., and M. Abdel-Mottaleb. 2021. A comparative study of deep learning models for diagnosing glaucoma from fundus images. *IEEE Access* 9:23894–906. doi:10.1109/ACCESS.2021.3056641.

Ambati, L. S., K, Narukonda, G. R. Bojja, and D. Bishop, 2020. Factors influencing the adoption of artificial intelligence in organizations - From an employee's perspective. MWAIS 2020 Proceedings.

Bojja, G. R., J. Liu, and L. Sai Ambati. 2021. Health information systems capabilities and Hospital performance – An SEM analysis. *AMCIS 2021 Proceedings* 31:1761.

Chan, K., T.-W. Lee, P. A. Sample, M. H. Goldbaum, R. N. Weinreb, and T. J. Sejnowski. 2002. Comparison of machine learning and traditional classifiers in glaucoma diagnosis. *IEEE Transactions on Bio-Medical Engineering* 49 (9):963–74. doi:10.1109/TBME.2002.802012.

Cheng, J., J. Liu, Y. Xu, F. Yin, D. W. K. Wong, N.-M. Tan, D. Tao, C.-Y. Cheng, T. Aung, and T. Y. Wong. 2013. Superpixel classification based optic disc and optic cup segmentation for glaucoma screening. *IEEE Transactions on Medical Imaging* 32 (6):1019–32. doi:10.1109/TMI.2013.2247770.

Civit-Masot, J., M. J. Domínguez-Morales, S. Vicente-Díaz, and A. Civit. 2020. Dual machine-learning system to aid glaucoma diagnosis using disc and cup feature extraction. *IEEE Access* 8:127519–29. doi:10.1109/ACCESS.2020.3008539.

Elangovan, P., and M. K. Nath. 2021. A novel shallow ConvNet-18 for malaria parasite detection in thin blood smear images. *SN Computer Science* 2 (5):1–11. doi:10.1007/s42979-021-00763-w.

Elangovan, P., and M. K. Nath. 2022. En-ConvNet: A novel approach for glaucoma detection from color fundus images using ensemble of deep convolutional neural networks. *International Journal of Imaging Systems and Technology* 32 (6):2034–48.

George, Y., B. J. Antony, H. Ishikawa, G. Wollstein, J. S. Schuman, and R. Garnavi. 2020. Attention-guided 3D-CNN framework for glaucoma detection and structural-functional association using volumetric images. *IEEE Journal of Biomedical and Health Informatics* 24 (12):3421–30. doi:10.1109/JBHI.2020.3001019.

Guo, F., Y. Mai, X. Zhao, X. Duan, Z. Fan, B. Zou, and B. Xie. 2018. Yanbao: A mobile app using the measurement of clinical parameters for glaucoma screening. *IEEE Access* 6:77414–28. doi:10.1109/ACCESS.2018.2882946.

Islam, M. T., S. T. Mashfu, A. Faisal, S. C. Siam, I. T. Naheen, and R. Khan. 2022. Deep learning-based glaucoma detection with cropped optic cup and disc and blood vessel segmentation. *IEEE Access* 10:2828–41. doi:10.1109/ACCESS.2021.3139160.

Kar, M. K., D. R. Neog, and M. K. Nath. 2022. Retinal vessel segmentation using multi-scale residual convolutional neural network (MSR-Net) combined with generative adversarial networks. *Circuits, Systems, and Signal Processing*. doi:10.1007/s00034-022-02190-5.

Kim, P. Y., K. M. Iftekharuddin, P. G. Davey, M. Tóth, A. Garas, G. Holló, and E. A. Essock. 2013. Novel fractal feature-based multiclass glaucoma detection and progression prediction. *IEEE Journal of Biomedical and Health Informatics* 17 (2):269–76. doi:10.1109/TITB.2012.2218661.

Li, L., M. Xu, H. Liu, Y. Li, X. Wang, L. Jiang, Z. Wang, X. Fan, and N. Wang. 2020. A large-scale database and a CNN model for attention-based glaucoma detection. *IEEE Transactions on Medical Imaging* 39 (2):413–24. doi:10.1109/TMI.2019.2927226.

Liao, W., B. Zou, R. Zhao, Y. Chen, Z. He, and M. Zhou. 2020. Clinical interpretable deep learning model for glaucoma diagnosis. *IEEE Journal of Biomedical and Health Informatics* 24 (5):1405–12. doi:10.1109/JBHI.2019.2949075.

Luo, X., J. Li, M. Chen, X. Yang, and X. Li. 2021. Ophthalmic disease detection via deep learning with a novel mixture loss function. *IEEE Journal of Biomedical and Health Informatics* 25 (9):3332–9. doi:10.1109/JBHI.2021.3083605.

Ma, Y., R. Fallahzadeh, and H. Ghasemzadeh. 2016. Glaucoma-specific gait pattern assessment using body-worn sensors. *IEEE Sensors Journal* 16 (16):6406–15. doi:10.1109/JSEN.2016.2582083.

Maheshwari, S., R. B. Pachori, and U. R. Acharya. 2017. Automated diagnosis of glaucoma using empirical wavelet transform and correntropy features extracted from fundus images. *IEEE Journal of Biomedical and Health Informatics* 21 (3):803–13. doi:10.1109/JBHI.2016.2544961.

Mary, M., E. B. Rajsingh, and G. R. Naik. 2016. Retinal fundus image analysis for diagnosis of glaucoma: A comprehensive survey. *IEEE Access* 4:4327–54. doi:10.1109/ACCESS.2016.2596761.

Mirjalili, S., S. M. Mirjalili, and A. Lewis. 2014. Grey wolf optimizer. *Advances in Engineering Software* 69:46–61. doi:10.1016/j.advengsoft.2013.12.007.

Moazzeni, A. R., and E. Khamehchi. 2020. Rain optimization algorithm (ROA): A new metaheuristic method for drilling optimization solutions. *Journal of Petroleum Science and Engineering* 195:107512.

Nath, M. K., and S. Dandapat, 2012. Differential entropy in wavelet sub-band for assessment of glaucoma. *International Journal of Imaging Systems and Technology* 22 (3):161–65.

Nawaz, M., T. Nazir, A. Javed, U. Tariq, H.-S. Yong, M. A. Khan, and J. Cha. 2022. An efficient deep learning approach to automatic glaucoma detection using optic disc and optic cup localization. *Sensors* 22 (2):434. doi:10.3390/s22020434.

Nayak, D. R., D. Das, B. Majhi, S. V. Bhandary, and U. R. Acharya. 2021. ECNet: An evolutionary convolutional network for automated glaucoma detection using fundus images. *Biomedical Signal Processing and Control* 67:102559. doi:10.1016/j.bspc.2021.102559.

Niwas, S. I., W. Lin, C. K. Kwoh, C.-C. J. Kuo, C. C. Sng, M. C. Aquino, and P. T. K. Chew. 2016. Cross-examination for angle-closure glaucoma feature detection. *IEEE Journal of Biomedical and Health Informatics* 20 (1):343–54. doi:10.1109/JBHI.2014.2387207.

Ovreiu, S., E.-A. Paraschiv, and E. Ovreiu. 2021. Deep learning & digital fundus images: Glaucoma detection using DenseNet. 13th International Conference on Electronics, Computers and Artificial Intelligence (ECAI), 1–4.

Parashar, D., and D. Agrawal. 2021a. 2-D compact variational mode decomposition-based automatic classification of glaucoma stages from fundus images. *IEEE Transactions on Instrumentation and Measurement* 70:1–10. doi:10.1109/TIM.2021.3071223.

Parashar, D., and D. K. Agrawal. 2020. Automated classification of glaucoma stages using flexible analytic wavelet transform from retinal fundus images. *IEEE Sensors Journal* 20 (21):12885–94. doi:10.1109/JSEN.2020.3001972.

Parashar, D., and D. K. Agrawal. 2021b. Automatic classification of glaucoma stages using two-dimensional tensor empirical wavelet transform. *IEEE Signal Processing Letters* 28:66–70. doi:10.1109/LSP.2020.3045638.

Patel, A. S., and V. Singh. 2021. Glaucoma detection using mask region-based convolutional neural networks. 5th International Conference on Electronics, Communication, and Aerospace Technology (ICECA), 1642–7.

Pedersen, M. E. H., and A. J. Chipperfield. 2010. Simplifying particle swarm optimization. *Applied Soft Computing* 10 (2):618–28. doi:10.1016/j.asoc.2009.08.029.

Serener, A., and S. Serte. 2019. Transfer learning for early and advanced glaucoma detection with convolutional neural networks. 2019 Medical Technologies Congress (TIPTEKNO), 1–4.

Shyamalee, T., and D. Meedeniya. 2022. CNN based fundus images classification For glaucoma identification. 2022 2nd International Conference on Advanced Research in Computing (ICARC).

Shyamalee, T., and D. Meedeniya. 2022b. Attention U-Net for glaucoma identification using fundus image segmentation. International Conference on Decision Aid Sciences and Applications (DASA), 6–10.

Shyamalee, T., and D. Meedeniya. 2022c. Glaucoma detection with retinal fundus images using segmentation and classification. *Machine Intelligence Research* 19 (6):563–80. doi:10.1007/s11633-022-1354-z.

Song, D., B. Fu, F. Li, J. Xiong, J. He, X. Zhang, and Y. Qiao. 2021a. Deep relation transformer for diagnosing glaucoma with optical coherence tomography and visual field function. *IEEE Transactions on Medical Imaging* 40 (9):2392–402. doi:10.1109/TMI.2021.3077484.

Song, W. T., I.-C. Lai, and Y.-Z. Su. 2021b. A statistical robust glaucoma detection framework combining retinex, CNN, and DOE using fundus images. *IEEE Access* 9:103772–83. doi:10.1109/ACCESS.2021.3098032.

Soni, M., I. R. Khan, K. S. Babu, S. Nasrullah, A. Madduri, and S. A. Rahin. 2022. Light weighted healthcare CNN model to detect prostate cancer on multiparametric MRI. *Computational Intelligence and Neuroscience* 2022:1–11. doi:10.1155/2022/5497120.

Sreng, S., N. Maneerat, K. Hamamoto, and K. Y. Win. 2020. Deep learning for optic disc segmentation and glaucoma diagnosis on retinal images. *Applied Sciences* 10 (14):4916.

Sudhan, M. B., M. Sinthuja, S. P. Raja, J. Amutharaj, G. C. P. Latha, S. S. Rachel, T. Anitha, T. Rajendran, and Y. A. Waji. 2022. Segmentation and classification of glaucoma using U-Net with deep learning model. *Journal of Healthcare Engineering* 2022:1–10. doi:10.1155/2022/1601354.

Tabassum, M., T. M. Khan, M. Arsalan, S. S. Naqvi, M. Ahmed, H. A. Madni, and J. Mirza. 2020. CDED-Net: Joint segmentation of optic disc and optic cup for glaucoma screening. *IEEE Access* 8:102733–47. doi:10.1109/ACCESS.2020.2998635.

Venugopal, V., J. Joseph, M. V. Das, and M. K. Nath. 2022a. An EfficientNet-based modified sigmoid transform for enhancing dermatological macro-images of melanoma and nevi skin lesions. *Computer Methods and Programs in Biomedicine* 222:106935. doi:10.1016/j.cmpb.2022.106935.

Venugopal, V., J. Joseph, M. V. Das, and M. K. Nath. 2022b. DTP-Net: A convolutional neural network model to predict threshold for localizing the lesions on dermatological macro-images. *Computers in Biology and Medicine: Elsevier (IF - 6.698, indexed in SCI)* 148:105852. doi:10.1016/j.compbiomed.2022.105852.

Vermeer, K. A., F. M. Vos, B. Lo, Q. Zhou, H. G. Lemij, A. M. Vossepoel, and L. J. van Vliet. 2006. Modeling of scanning laser polarimetry images of the human retina for progression detection of glaucoma. *IEEE Transactions on Medical Imaging* 25 (5):517–28. doi:10.1109/TMI.2006.871433.

Yousefi, S., M. H. Goldbaum, M. Balasubramanian, T.-P. Jung, R. N. Weinreb, F. A. Medeiros, L. M. Zangwill, J. M. Liebmann, C. A. Girkin, and C. Bowd. 2014. Glaucoma progression detection using structural retinal nerve fiber layer measurements and functional visual field points. *IEEE Transactions on Bio-Medical Engineering* 61 (4):1143–54. doi:10.1109/TBME.2013.2295605.

Yuan, Z., W. Wang, H. Wang, and A. Yildizbasi. 2020. Developed Coyote Optimization Algorithm and its application to optimal parameters estimation of PEMFC model. *Energy Reports* 6:1106–17. doi:10.1016/j.egyr.2020.04.032.

Zhao, R., X. Chen, X. Liu, Z. Chen, F. Guo, and S. Li. 2020. Direct cup-to-disc ratio estimation for glaucoma screening via semi-supervised learning. *IEEE Journal of Biomedical and Health Informatics* 24 (4):1104–13. doi:10.1109/JBHI.2019.2934477.

Zotin, A. 2018. Fast algorithm of image enhancement based on multi-scale retinex. *Procedia Computer Science* 131:6–14. doi:10.1016/j.procs.2018.04.179.